

The Early Eocene Ekmekçi granodiorite porphyry in the Karacabey region (Sakarya Zone, NW Turkey)

Gürsel SUNAL^{1*}, Mehmet Korhan ERTURAÇ², Gültekin TOPUZ³, Aral I. OKAY^{1,3}, Thomas ZACK⁴

¹Department of Geology, Faculty of Mines, İstanbul Technical University, İstanbul, Turkey

²Department of Geography, Faculty of Arts and Sciences, Sakarya University, Esentepe Campus, Serdivan, Sakarya, Turkey

³Eurasia Institute of Earth Sciences, İstanbul Technical University, Maslak, İstanbul, Turkey

⁴Department of Earth Sciences, University of Gothenburg, Gothenburg, Sweden

Received: 09.11.2018 • Accepted/Published Online: 28.04.2019 • Final Version: 22.07.2019

Abstract: The Ekmekçi granodiorite porphyry is a unit in the E-W trending, postcollisional Eocene magmatic rocks of northern Anatolia. It occurs as a relatively small stock, but represents a link between plutonic and volcanic rocks. This Early Eocene granodiorite porphyry intruded into the Upper Triassic rocks of the Karakaya complex in the Sakarya Zone. In this study we present geochemical and zircon U-Pb LA-ICP-MS age data to contribute to understanding the Early Tertiary postcollisional tectonic setting of NW Anatolia. The granodiorite porphyry includes plagioclase, quartz, hornblende, K-feldspar, biotite, and minor zircon, apatite, sphene, and opaque minerals. The stock displays medium-K calc-alkaline I-type and metaluminous affinity. Similar to other Eocene magmatic rocks, it displays characteristic features of subduction-related magmatism, such as enrichment in large-ion lithophile elements relative to high-field strength elements and enrichment of light rare earth elements relative to heavy rare earth elements with a lack of significant Eu anomalies. They are characterized by homogeneous initial Sr and Nd isotopic compositions of 0.7044–0.7049 and 0.51255–0.51260, respectively. Zircon U-Pb data indicate that the Ekmekçi granodiorite porphyry was emplaced at 5.1 ± 1 Ma (2s Ypresian). Geochemically, the Ekmekçi granodiorite porphyry is similar to mafic volcanic rocks rather than the plutonic rocks of the same age. It was emplaced to the north of the İzmir-Ankara-Erzincan Suture (northern plutonic belt of NW Anatolia) and can be correlated with southern plutons such as Orhaneli, Topuk, Tepeldağ, Gürgenyayla, and Sivrihisar in the Anatolide-Tauride block in terms of age.

Key words: Early Eocene granodiorite porphyry, Sakarya Zone, NW Turkey, geochemistry, U-Pb zircon age

1. Introduction

Following the Late Cretaceous northward subduction of the Neotethyan Ocean under the Pontides, the Sakarya Zone and the Anatolide-Tauride Block were amalgamated during Paleocene time and the İzmir-Ankara-Erzincan Suture Zone (İAESZ) formed (Şengör and Yılmaz, 1981; Okay and Tüysüz, 1999). The Middle Eocene clastic and volcanic rocks cover all the pre-Eocene units with a pronounced unconformity along a roughly E-W trending belt of ≥ 1000 km in length north of the İAESZ (Harris et al., 1994; Keskin et al., 2008; Topuz et al. 2011; Altunkaynak and Dilek, 2013). Mainly turbiditic sediments filled the intermountain basins. Even though the Eocene is the time of the last marine sedimentation in the region, collision-related compression lasted up until the Miocene (see Sunal and Erturaç, 2012, and the references therein and Özdamar et al., 2018).

Although the Eocene volcanic rocks developed along an almost continuous E-W belt (Figure 1), plutonic and

subvolcanic rocks are concentrated mainly in the western and eastern parts of the belt. They have various sizes and are represented by plutons, stocks, and sills, and they show generally calc-alkaline (rarely high-K and shoshonitic), metaluminous to peraluminous I-type geochemical affinities. The Eocene magmatism with adakitic and nonadakitic signature is reported from both western and eastern parts of northern Anatolia (Topuz et al., 2005, 2011; Karlı et al., 2010, 2011; Eyüboğlu et al., 2011; Altunkaynak et al., 2012; Dokuz et al., 2013).

The Ekmekçi granodiorite porphyry in the Karacabey region is located in the western Sakarya Zone (Figure 1). Its age was given as Paleozoic in a previous study because the metamorphic country rocks of the Ekmekçi granodiorite porphyry were thought to be of Paleozoic age (Ergül et al., 1986). However, later studies have shown that the metamorphism in the country rocks is of Late Triassic age (Okay and Monié, 1997), which conclusively indicates that the Ekmekçi granodiorite porphyry cannot be

* Correspondence: gsunal@itu.edu.tr

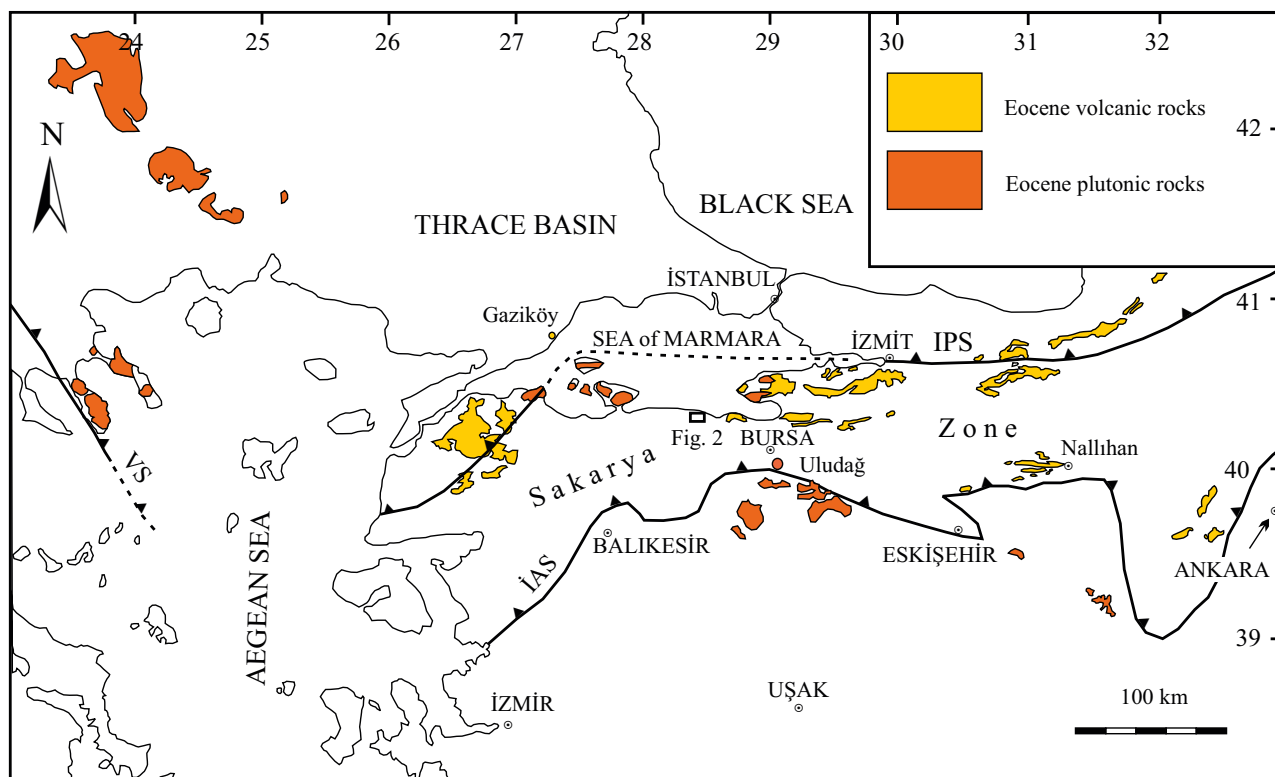


Figure 1. Map showing the distribution of Eocene plutonic and volcanic rocks in the northeast Aegean region. Sources: Kürkcüoğlu et al. (2008), Altunkaynak et al. (2012) and the references therein, Altunkaynak and Dilek (2013), Gülmez et al. (2013), Ersoy and Palmer (2013), Kasapoğlu et al. (2016), Topuz and Okay (2017).

Paleozoic in age. In this study, we present the zircon U-Pb age and major trace element and Sr-Nd isotope data from this granodiorite porphyry to provide information about its emplacement history and the Cenozoic postcollisional tectonomagmatic evolution of the NW Sakarya Zone.

2. Geological setting

The Sakarya Zone is an E-W trending belt bounded by the Intra-Pontide suture to the north and the İzmir-Ankara-Erzincan suture to the south (Okay and Tüysüz, 1999; Figure 1). The Sakarya Zone has a composite basement comprising Paleozoic and Permo-Triassic crystalline rocks, which are unconformably overlain by Jurassic and younger sedimentary units (Okay and Tüysüz, 1999; Okay and Göncüoğlu, 2004; Okay et al., 2006). The oldest rocks are represented by low-grade metamorphic rocks of unknown age, which were intruded by Devonian granites (Okay et al., 1994, 2006; Aysal et al., 2012b, 2012b; Sunal, 2012). Another basement type is reworked Paleozoic high-grade metamorphic rocks reported both from the western and the central Sakarya Zone. The Kazdağ Massif in the western Sakarya Zone is made up of amphibolite-facies paragneiss, orthogneiss,

schists, marble, and metaophiolites (Okay et al., 1996; Duru et al., 2004; Cavazza et al., 2009). The essential part of the pre-Jurassic basement is represented by Early Carboniferous high-temperature/middle to low-pressure metamorphic rocks exposed in the Pular, Kurtuluş, and Sarıcakaya areas (Topuz and Altherr, 2004; Topuz et al., 2004, 2007). These are intruded by Carboniferous granitoids (Topuz et al., 2010; Dokuz, 2011; Kaygusuz et al., 2012; Ustaömer et al., 2012). The Permo-Triassic low-grade metamorphic rocks, which are commonly interpreted as accretionary complexes and known as the Karakaya Complex, represent another group of basement units. They include greenschist- to blueschist-facies metabasite, phyllite, marble and minor metachert, and tectonic slices of serpentinite. The metabasites include at least one tectonic lens of Triassic eclogite dated at 205 ± 3 Ma (Okay and Monié, 1997). Moreover, there are tectonic slices of Middle Permian ophiolite (Topuz et al., 2018). In the Karacabey region, these basement units are unconformably overlain by Jurassic sandstone and carbonate (Ergül et al., 1986; Altınır, 1991; Sunal, 2012; Aysal et al., 2012a). Besides those direct occurrences of pre-Jurassic basements in the Sakarya Zone, a wide range

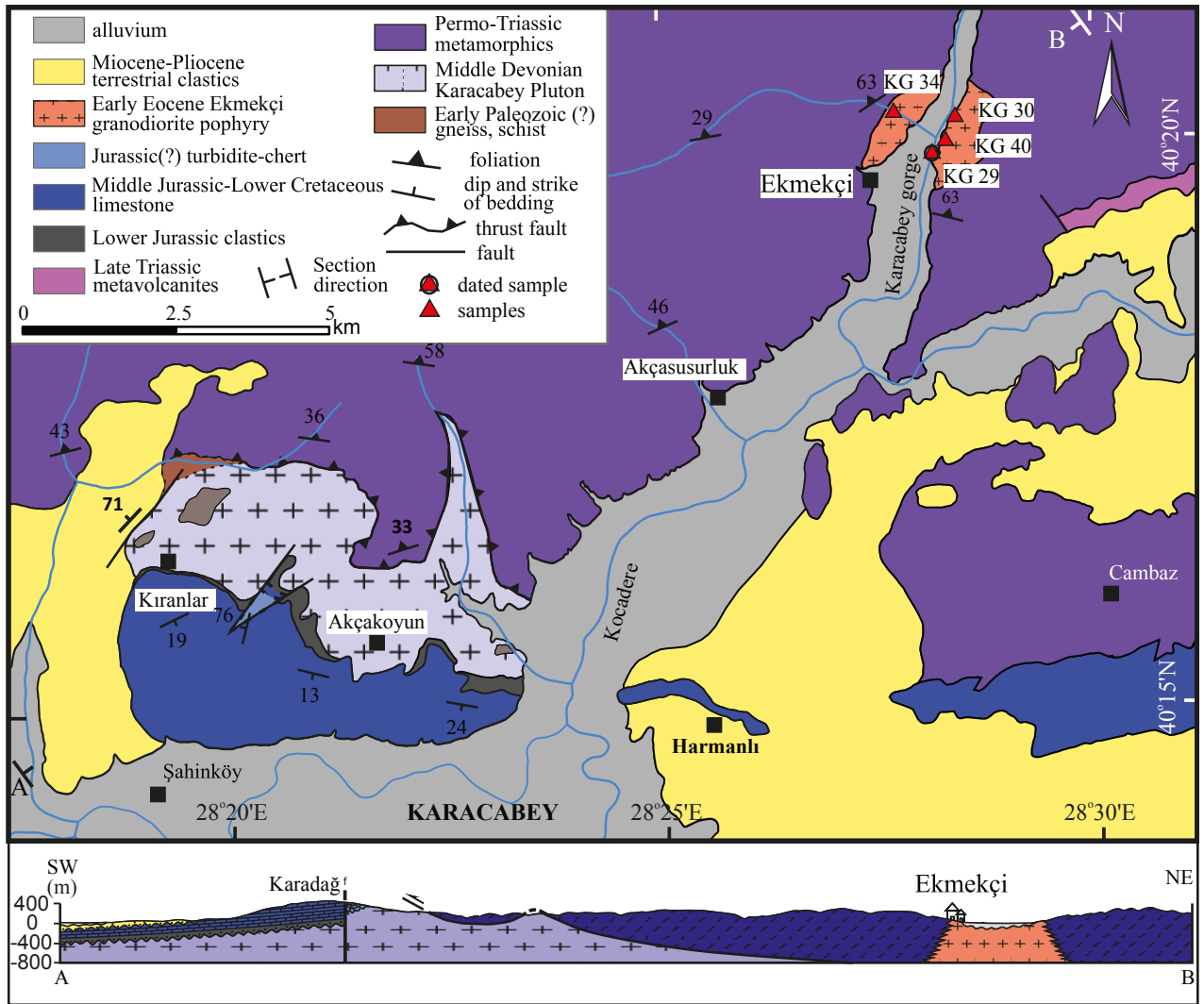


Figure 2. Geological map of the Karacabey Region (modified after Ergül et al., 1986 and Sunal, 2012).

of pre-Jurassic detrital zircon ages revealing the complete basement history of the Sakarya Zone was reported (Akdoğan et al., 2018; Şengün and Koralay, 2019).

The Ekmekçi granodiorite porphyry is a small stock, which intrudes into the metamorphic rocks of the Lower Karakaya Complex (Figure 2). This shallow-level intrusion, which was considered as a part of the Karacabey pluton in previous studies (Ergül et al., 1986), is dated as Early Eocene here.

3. Analytical techniques

3.1. Whole-rock analyses

The whole-rock powders were split from 1–5 kg of crushed rocks. Whole-rock analyses were performed at Acme Analytical Laboratories Ltd. in Vancouver, Canada. Rock powder of 200 mg was mixed with 1.5 g of LiBO_2 flux in a graphite crucible. Subsequently, the crucible was placed in an oven and heated to 1050 °C for 15 min. The molten

samples were dissolved in 5% HNO_3 (ACS grade nitric acid diluted in demineralized water). International reference samples and reagent blanks were added to the sample sequence. For analyses of major elements and the trace elements Ba, Nb, Ni, Sr, Sc, Y, and Zr, sample solutions were aspirated into an ICP atomic emission spectrograph (Jarrel Ash AtomComb 975). For the determination of other trace elements including rare earth elements, the solutions were aspirated into an ICP mass spectrometer (PerkinElmer Elan 6000). Accuracy was better than 2% for major and better than 10% for trace elements.

3.2. Sr-Nd isotope analyses

Isotope ratio measurements were performed on the Finnigan MAT 262 TIMS of the Isotope Geochemistry Group of the University of Tübingen (Germany). Sample powders were weighed into Teflon beakers and mixed with adequate amounts of tracer solutions enriched in

$^{87}\text{Rb}/^{84}\text{Sr}$ and $^{149}\text{Sm}/^{150}\text{Nd}$, respectively. Digestion was achieved via HF (48%)-HNO₃ (65%) acid attack by placing the closed beakers on a hot plate at 140 °C. Digested samples were dried and transformed to chlorides in 6 N HCl. The samples were then redissolved in 2.5 N HCl for chromatographic separation. Rb, Sr, and light rare earth elements were purified by conventional ion exchange chromatography using quartz glass columns filled with Bio-Rad AG 50W-X12 (200–400 mesh). Subsequent separation of Sm and Nd was achieved using a reverse ion chromatographic procedure using quartz glass columns filled with HDEHP resin (Richard et al., 1976). Sr separates were loaded with a Ta-activator on W single filaments and isotope ratio measurements were performed in dynamic mode. Rb was loaded on Re double filaments. Analytical mass fractionation was corrected using a $^{88}\text{Sr}/^{86}\text{Sr}$ ratio of 8.375209 and exponential law. Long-term reproducibility for NBS SRM 987 (n = 30) is 0.710248 ± 11 for the $^{87}\text{Sr}/^{86}\text{Sr}$ ratio. Total procedural blanks (chemistry and loading) were <450 pg for Sr and <15 pg for Rb. Sm and Nd were loaded as phosphate on Re double filaments and measured in static multiple collector mode. Analytical mass fractionation was corrected with $^{146}\text{Nd}/^{144}\text{Nd}$ of 0.7219 using exponential law. Repeated measurements of the La Jolla Nd standard (n = 12) gave a $^{143}\text{Nd}/^{144}\text{Nd}$ ratio of 0.511838 ± 13 . Procedural blanks were <90 pg for Nd and <20 pg for Sm.

3.3. Zircon U-Pb LA-ICP-MS technique

Zircons were extracted from rock samples by standard mineral separation techniques with crushing, sieving, Frantz isodynamic magnetic separation, and heavy liquids and were finally handpicked under a binocular microscope. A fraction with grain sizes of 63–200 µm was then classified according to crystal properties (i.e. euhedral morphology, lack of overgrowth, and visible inclusions). The grains were mounted in epoxy resin, polished, and imaged using cathodoluminescence (CL) on a Zeiss Evo 50 EP scanning electron microscope at Hacettepe University in Ankara.

LA-ICP-MS analyses for the zircons were performed at the Institute of Geosciences at Johannes Gutenberg University Mainz, utilizing a system consisting of a New Wave 213 nm laser coupled to an Agilent 7500ce quadrupole ICP-MS. Analytical procedures are the same as outlined by Topuz et al. (2010, 2011). Final age calculation was performed using the computer program Isoplot 3.0 (Ludwig, 2003).

4. Results

4.1. Petrography of the Early Eocene Ekmekçi granodiorite porphyry

The Ekmekçi granodiorite porphyry consists of plagioclase (>40 vol.%), K-feldspar (~10 vol.%), quartz (~25 vol.%), hornblende (~10 vol.%), and biotite (~5 vol.%)

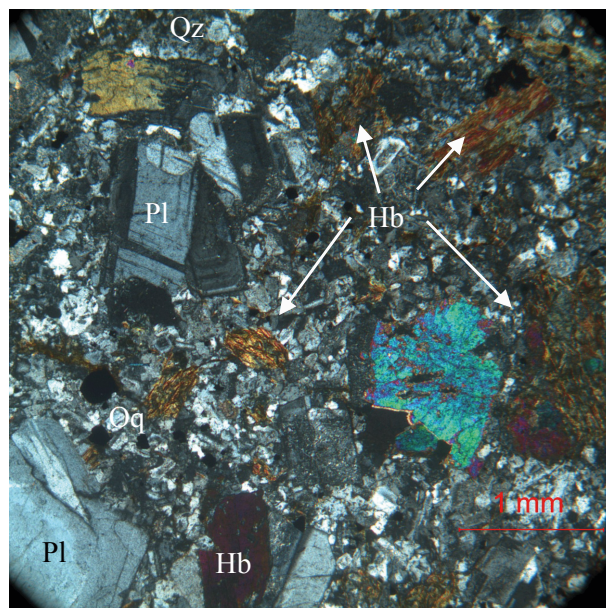


Figure 3. Cross-polarized thin-section photomicrograph of hornblende-rich granodiorite porphyry (KG29). Pl: Plagioclase, Qz: quartz, Hb: hornblende, Opq: opaque minerals.

phenocrysts set in a fine-grained groundmass of the same minerals (Figure 3). Idiomorphic plagioclase phenocrysts are often corroded by fine-grained plagioclase grains in the groundmass and occasionally contain inclusions of magnetite, apatite, zircon, and titanite. Hornblende occurs as elongate euhedral crystals. Biotite is represented by elongated and small crystals. Titanite is always associated with the opaque phase. Zircon and apatite occur generally as inclusions in plagioclase and biotite.

4.2. U-Pb zircon dating

Sample KG29 from the granodiorite porphyry was dated using the zircon U-Pb LA-ICP-MS method (Figure 2). Figure 4 shows cathodoluminescence (CL) images of the zircons extracted from sample KG29. All analyzed zircons have perfect internal oscillatory zoning indicating their magmatic origin. Sector zoning is also a common feature for the zircons. Inheritance is not clear in the CL photographs.

In total, 21 spots were analyzed (Table 1). The ages are concordant or slightly discordant (Figure 5). Only seven analyses are concordant (between 90–110%). $^{206}\text{Pb}/^{238}\text{U}$ ages of the spots range between 47 and 54 Ma (Table 1). On a Tera-Wasserburg plot, a lower intercept age of 50.9 ± 1.2 Ma (2 s) (Ypresian, Early Eocene) was obtained (Figure 5), which is interpreted as the crystallization age of the Ekmekçi granodiorite porphyry.

4.3. Major and trace element geochemistry

A total of 4 samples from the Ekmekçi granodiorite porphyry were analyzed for their major and trace element

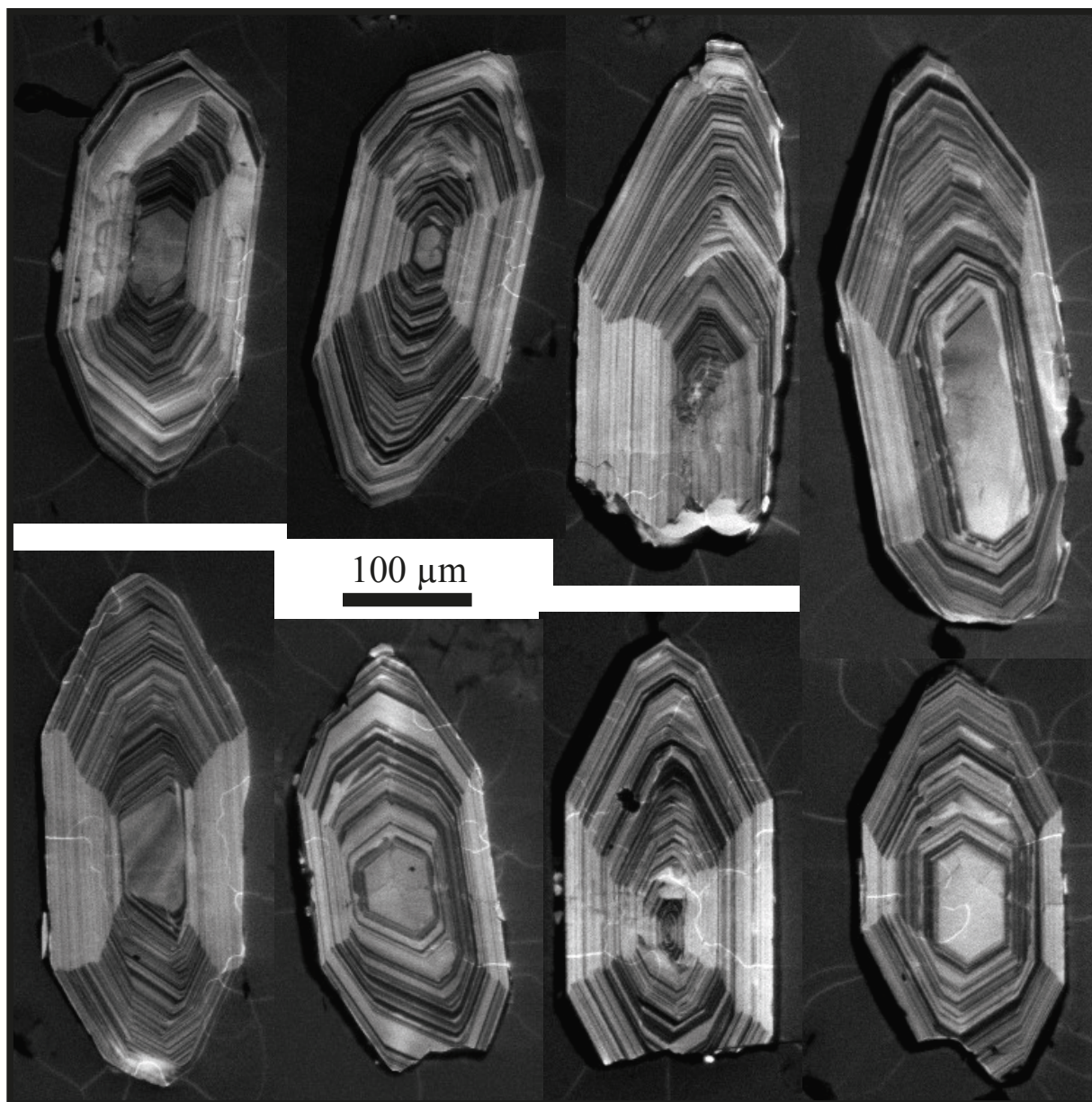


Figure 4. Cathodoluminescence (CL) images of the zircons extracted from sample KG29. All grains have oscillatory magmatic zoning and are free of inheritance. For ages, see Table 1.

compositions (Table 2; Figure 2). Petrographic features of the analyzed samples are similar (see Section 4.1).

The chemical compositions of the samples fall into the granodiorite and quartz diorite fields on SiO_2 versus total alkali diagrams (Figure 6; Middlemost, 1985). In AFM and SiO_2 versus K_2O classifications (Figure 7a; Irvine and Baragar, 1971; Peccerillo and Taylor, 1976), they plot in the field of calc-alkaline series except for one sample, which falls into the tholeiite series (Figure 7b). All the samples lie in the metaluminous, I-type field of Shand (1943) (Figure 7c).

SiO_2 abundances of the samples vary in a narrow range between 64 and 66 wt.% (Table 2). TiO_2 , Al_2O_3 , MgO , CaO , and Na_2O concentrations also vary in a narrow range. The $\text{Fe}_2\text{O}_3^{\text{tot}}$ concentration is slightly higher in sample KG34 than in other samples (western sample). The Mg# ranges from 36 to 41 (Table 2).

Chondrite-normalized rare earth element (REE) patterns of the samples show slight HREE (heavy rare earth elements: Dy to Lu) concave upward shapes (Figure 8). Furthermore, they are characterized by slight negative Eu anomalies (Eu/Eu^* is ~ 0.86 ; Table 2; Figure 8),

Table 1. U-Pb zircon geochronological data of sample KG29.

Spot	U (ppm)	Th (ppm)	Th/U	²⁰⁷ Pb/ ²³⁵ U	²⁰⁶ Pb/ ²³⁸ U	rho	²⁰⁷ Pb/ ²⁰⁶ Pb	²⁰⁸ Pb/ ²³² Th	²⁰⁷ Pb/ ²³⁵ U	Apparent ages (Ma)		Concordance
										²⁰⁶ Pb/ ²³⁸ U	²⁰⁸ Pb/ ²³² Th	
1	385	190	0.49	0.057(05)	0.0079(03)	0.08	0.0548(053)	0.0022(03)	56.5 ± 5.2	50.5 ± 1.6	45.2 ± 6.1	89%
2	599	363	0.61	0.049(04)	0.0076(03)	0.33	0.0469(039)	0.0021(02)	48.6 ± 4.1	49.0 ± 1.6	41.8 ± 5.0	101%
3	401	175	0.44	0.053(05)	0.0079(29)	0.29	0.0496(043)	0.0022(03)	52.4 ± 4.7	50.5 ± 1.6	45.2 ± 6.1	96%
4	398	174	0.44	0.052(06)	0.0080(02)	0.02	0.0485(053)	0.0022(03)	51.6 ± 5.4	51.2 ± 2.3	43.5 ± 6.0	99%
5	452	260	0.57	0.053(05)	0.0079(02)	0.02	0.0503(056)	0.0021(03)	52 ± 5.3	50.5 ± 1.6	41.8 ± 5.8	97%
6	624	377	0.60	0.052(05)	0.0076(40)	0.40	0.0501(042)	0.0022(03)	51.7 ± 4.7	49.0 ± 1.6	45.2 ± 5.3	95%
7	500	275	0.55	0.069(10)	0.0082(02)	0.02	0.0654(096)	0.0029(05)	68.2 ± 9.1	52.9 ± 2.5	57.8 ± 9.7	78%
8	508	290	0.57	0.060(09)	0.0080(02)	0.02	0.0587(091)	0.0025(04)	59.5 ± 8.6	51.5 ± 2.5	50.4 ± 7.8	86%
9	389	147	0.38	0.063(12)	0.0082(05)	0.05	0.0588(116)	0.0023(04)	61.6 ± 11.5	52.9 ± 3.2	46.7 ± 9.0	86%
10	636	445	0.70	0.061(09)	0.0081(08)	0.08	0.0578(088)	0.0026(04)	60.2 ± 8.4	52.2 ± 3.2	52.2 ± 7.9	87%
11*	399	205	0.51	0.116(34)	0.0073(41)	-0.41	0.1339(471)	0.0052(17)	111 ± 31.2	47.1 ± 5.2	104.4 ± 33.5	42%
12	295	139	0.47	0.089(14)	0.0084(02)	0.02	0.0870(160)	0.0028(06)	86.3 ± 13.1	53.6 ± 3.2	56.0 ± 11.1	62%
13	351	182	0.52	0.056(10)	0.0079(22)	0.22	0.0576(105)	0.0026(05)	55.8 ± 10.1	50.8 ± 3.8	52.2 ± 9.3	91%
14	408	225	0.55	0.077(14)	0.0082(02)	0.02	0.0716(138)	0.0030(06)	75.6 ± 13.6	52.9 ± 3.2	59.7 ± 12.9	70%
15	223	87	0.39	0.062(15)	0.0079(02)	0.02	0.0625(160)	0.0032(07)	61.3 ± 14.3	50.8 ± 3.8	65.3 ± 13.2	83%
16	522	255	0.49	0.040(07)	0.0077(16)	0.16	0.0409(077)	0.0023(04)	39.8 ± 7.3	49.3 ± 3.1	46.7 ± 9.0	124%
17	529	277	0.52	0.035(07)	0.0084(02)	0.02	0.0327(066)	0.0024(04)	34.7 ± 6.5	53.6 ± 3.2	48.5 ± 7.6	155%
18	340	138	0.41	0.060(11)	0.0081(20)	0.20	0.0570(106)	0.0021(04)	59.1 ± 10.9	52.2 ± 3.2	42.9 ± 8.8	88%
19	365	152	0.42	0.047(09)	0.0085(13)	0.13	0.0441(081)	0.0030(06)	47 ± 8.4	54.4 ± 3.2	59.7 ± 11.3	116%
20	449	193	0.43	0.051(09)	0.0084(23)	0.23	0.0467(078)	0.0022(04)	50.8 ± 8.5	53.6 ± 3.2	44.8 ± 8.9	106%
21	474	221	0.47	0.053(10)	0.0082(02)	0.02	0.0511(108)	0.0024(05)	52.1 ± 9.4	52.9 ± 3.2	48.5 ± 9.1	102%

U and Th concentrations are estimated from sensitivity factors calculated from GJ zircon (the Mainz crystal has 322 ppm U and 10.7 ppm Th). ²³⁵U is calculated from ²³⁸U using a ²³⁸U/²³⁵U ratio of 137.88. rho = error correlation defined as the quotient of the propagated errors of the ²⁰⁶Pb/²³⁸U, ²⁰⁷Pb/²³⁵U, and ²⁰⁷Pb/²⁰⁶Pb ratios. Uncertainties in parentheses are given for the last two digits (three digits for ²⁰⁷Pb/²⁰⁶Pb) and correspond to 1σ. * = analysis is not used for age calculation due to anomalous ²⁰⁷Pb/²³⁵U ratio.

signifying no significant plagioclase fractionation during granodiorite formation. (La/Yb)_{cn} ratios are generally low (~5; Table 2), indicating slight fractionation of light REEs relative to middle REEs, while there is almost no fractionation of middle REEs relative to heavy REEs.

Primitive mantle-normalized element concentration diagrams of the granodiorites exhibit negative anomalies of Ta-Nb, P, and Ti relative to their adjacent large-ion lithophile elements (LILEs: Sr, K, Rb, Ba, and Th) and light rare earth elements (LREEs: La to Nd) (Figure 8).

4.4. Sr-Nd isotope geochemistry

Whole-rock Sr and Nd isotope data are listed in Table 3. Initial Nd and Sr isotopic compositions are recalculated to 51 Ma. All of the samples have similar initial ⁸⁷Sr/⁸⁶Sr and ¹⁴³Nd/¹⁴⁴Nd ratios of 0.70442–0.70496 and 0.51256–0.51260, respectively (Table 3; Figure 9). Initial epsilon

Nd values of the samples are generally positive (0.1 and 0.6), except for sample KG40, which has a slightly negative value (–0.3) (Table 3).

5. Discussion

5.1. Geological context during the late Cretaceous-Eocene interval in the Sakarya Zone

The Late Cretaceous history of northern Anatolia is marked by E-W trending arc-related magmatic rocks resulting from the northward subduction of the Neotethyan Ocean under the Pontides. The Paleocene corresponds to the main collision between the Anatolide-Tauride block and the Pontides (Şengör and Yılmaz, 1981; Okay et al., 1994; Okay and Tüysüz, 1999). The İAESZ formed as a result of this collision. The Eocene period is represented by postcollisional intermountain basin formation (Tüysüz and

Table 2. Whole-rock analyses of collected samples.

Sample	KG34	KG29	KG40	KG30
SiO ₂	64.0	65.0	66.1	65.4
TiO ₂	0.48	0.46	0.40	0.43
Al ₂ O ₃	16.94	17.24	16.80	16.85
Fe ₂ O ₃ ^{tot}	5.11	3.68	3.57	4.12
MnO	0.06	0.04	0.06	0.06
MgO	1.71	1.03	1.15	1.42
CaO	5.06	4.66	4.88	5.00
Na ₂ O	4.35	5.03	4.68	4.83
K ₂ O	1.30	1.65	1.53	0.99
P ₂ O ₅	0.16	0.16	0.14	0.15
LOI	1.08	1.08	0.73	0.89
Total	100.3	100.1	100.1	100.1
Ni	1.5	2.4	1.0	1.7
Co	5.6	5.6	5.4	3.4
V	61	59	48	58
Cu	3.5	11.9	16.2	1.9
Zn	32	16	15	15
Cs	1.3	0.1	0.3	0.1
Rb	30.4	19.4	30.7	16.9
Ba	325	251	343	350
U	2.1	1.7	1.4	2.1
Th	6.0	6.6	7.1	7.3
Pb	2.4	2.3	1.3	1.1
Sr	445.7	485.5	417.0	416.5
Nb	6.9	7.6	7.3	7.7
Ta	0.5	0.6	0.8	0.6
Zr	129.7	125.4	126.0	133.0
Hf	3.3	3.4	3.3	3.5
Y	23.4	23.1	22.8	22.1
Ga	16.4	16.2	17.2	17.0
La	21.2	23.0	23.5	20.0
Ce	40.9	42.1	47.6	40.0
Pr	4.49	4.73	4.92	4.38
Nd	17.8	18.3	18.9	17.3
Sm	3.34	3.99	3.76	3.64
Eu	1.03	1.15	1.06	1.01
Gd	4.00	4.22	3.65	3.48
Tb	0.62	0.66	0.60	0.59
Dy	3.91	4.66	3.72	3.71
Ho	0.82	0.88	0.86	0.78
Er	2.49	2.88	2.42	2.35
Tm	0.40	0.40	0.37	0.35
Yb	2.64	2.88	2.68	2.87
Lu	0.44	0.48	0.43	0.43
K ₂ O/Na ₂ O	0.30	0.33	0.33	0.20
Mg#	39.87	35.67	38.96	40.58
ASI	0.95	0.93	0.92	0.93
(La/Yb) _{cn}	5.41	5.38	5.91	4.70
Eu/Eu*	0.86	0.85	0.86	0.86

Mg# = $100 \times (\text{MgO}/(\text{MgO} + \text{FeO}^{\text{tot}}))$ in molar proportions.

ASI = aluminum saturation index = molar $\text{Al}_2\text{O}_3/(\text{CaO} + \text{Na}_2\text{O} + \text{K}_2\text{O})$.

(La/Yb)_{cn} = chondrite-normalized La/Yb ratio.

Eu/Eu* = $[\text{Eu}_{\text{cn}} / (\text{Sm}_{\text{cn}} \cdot \text{Gd}_{\text{cn}} \cdot 0.5)]$.

Oxides are given in wt.% trace elements in µg/g.

Dellaloğlu, 1992; Tüysüz et al., 1995). Almost everywhere in the Pontides, mostly along the İAESZ and the Intra-Pontide Suture Zone, Eocene flysch type sediments with extensive volcanic rocks unconformably overlie the older rocks (see Keskin et al., 2008 for a compilation). Furthermore, there are Eocene plutonic rocks of various shapes and sizes intruding into the pre-Paleocene units of the eastern Pontides, Sakarya, and Tavşanlı Zones in NW Anatolia (Harris et al., 1994; Köprübaşı and Aldanmaz., 2004; Topuz et al., 2005, 2011; Okay and Satır, 2006; Karacık et al., 2008; Ustaömer et al., 2009; Karlı et al., 2011; Altunkaynak et al., 2012; Ersoy and Palmer, 2013; Topuz and Okay, 2017).

During Oligocene time a regional exhumation took place (Hejl et al., 2010; Cavazza et al., 2012) and the whole of the Pontides, except the westernmost part (northern and eastern part of the Thrace basin; Less et al., 2011; Okay et al. 2019), was uplifted above sea level. Thus, the Eocene sediments represent the last marine deposits in most of the Pontides.

5.2. Eocene magmatism in the Sakarya Zone

The Paleocene in the Pontides is represented by collisional events and marks the end of the subduction-related magmatism related to the İzmir-Ankara-Erzincan ocean. Therefore, Eocene magmatism is considered postcollisional with respect to closure time of the İzmir-Ankara-Erzincan suture (Harris et al., 1994). Even if there is a consensus about the postcollisional nature of the Eocene magmatism in the region, there are different ideas about the genesis of Eocene magmatism. For example, some researchers claim that the Eocene magmatism in northwest Turkey is related to subduction along the branches of the Tethys (Okay and Satır, 2006; Ustaömer et al., 2009). In the western Sakarya Zone, Okay and Satır (2006) attributed the arc-like geochemical signature of the plutonic rocks south of the İAESZ to the NE-vergent subduction along the Hellenic subduction zone. Furthermore, Ustaömer et al. (2009) assigned a middle Eocene sill of Marmara Island to a magmatic arc that postdates suturing and was emplaced in the early stages of mountain building. In the Eastern Pontides, Eyüboğlu et al. (2011) claimed that the Eocene magmatic rocks they investigated represented subduction-related adakitic magmas based on the geochemical characteristics of the rocks. They proposed southward subduction of the Tethys Ocean in the present-day Black Sea basin. However, there is a general consensus about the postcollisional character of the Eocene magmatic rocks with respect to the İAESZ because of the well-known nature of the geological basement of the Pontides and occurrence of Eocene plutonic and volcanic rocks both to the north and south of the İAESZ. This is in clear contradiction to the distribution of Late Cretaceous magmatic rocks, which are confined to the north of the İAESZ.

In the western Sakarya Zone and also in the southern

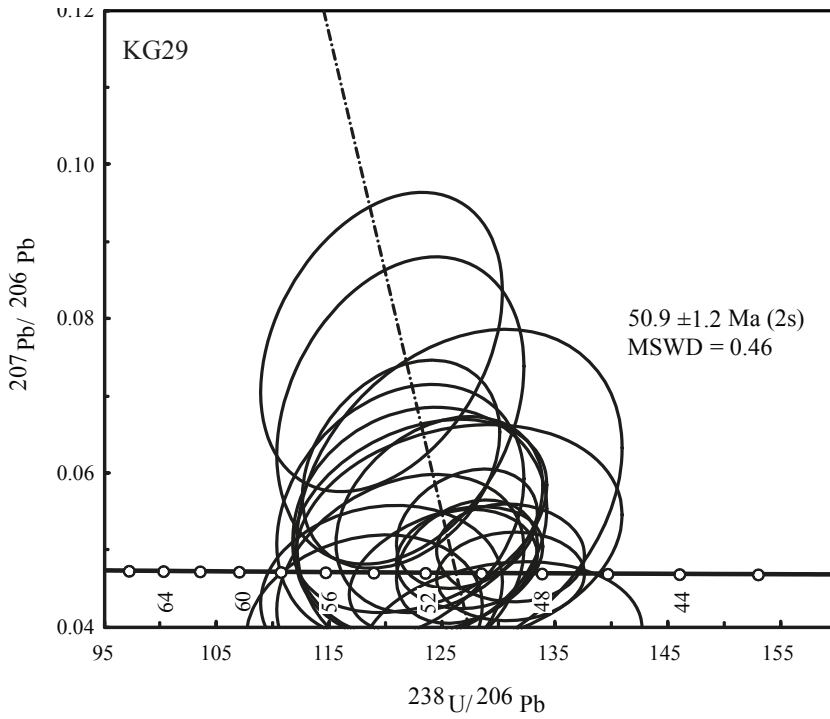


Figure 5. Tera-Wasserburg plot of zircons from dated sample KG29 (Isoplot 3.0, Ludwig, 2003).

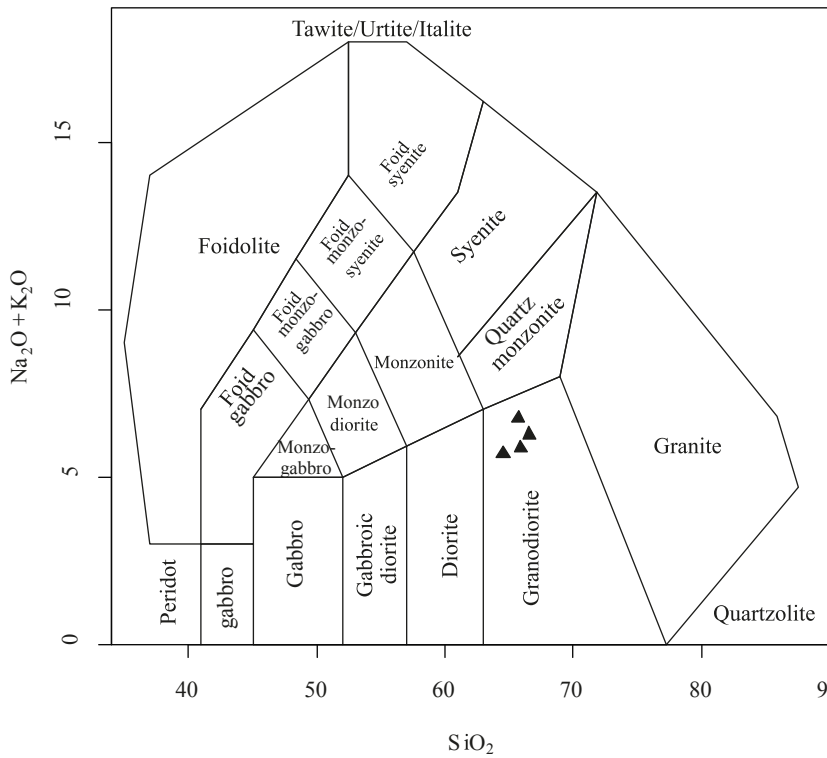


Figure 6. Geochemical nomenclature of the samples from the Ekmekçi granodiorite porphyry on total alkali vs. SiO₂ diagrams of Middlemost (1985). All of the samples fall into the granodiorite fields.

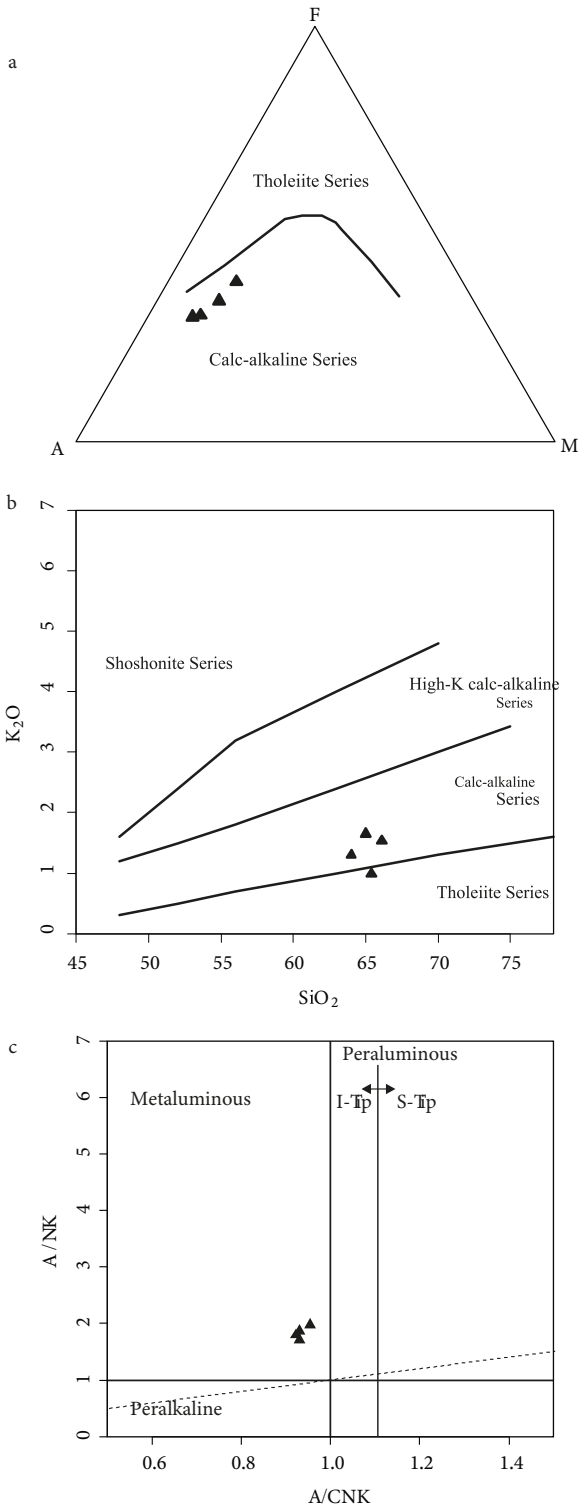


Figure 7. The distribution of the samples on the AFM diagram of Irvine and Baragar (1971), K_2O - SiO_2 diagram of Peccerillo and Taylor (1976), and A/NK vs. A/CNK diagram of Shand (1943). All samples belong to the medium-K, calc-alkaline series except one in the tholeiite series on the K_2O - SiO_2 diagram of Peccerillo and Taylor (1976).

part of the İstanbul Zone, Eocene plutonic rocks are classified according to their position relative to the İAESZ. Altunkaynak et al. (2012) described two distinct zones within the northern Neotethys suture zone, namely the northern and southern belts. The northern belt is slightly older (52–45 Ma) than the southern one (47–36 Ma). They also stated that the northern belt granitoids have inherited zircons, indicating more continental crust involvement in magma generation. The rocks of the southern belt are calc-alkaline to high-K calc-alkaline (Köprübaşı and Aldanmaz, 2004; Okay and Satır, 2006; Karacık et al., 2008; Çelebi and Köprübaşı, 2014), except some syenites from the Orhaneli Pluton, which are alkaline in nature (shoshonitic; Altunkaynak et al., 2012). Some of the high-K calc-alkaline varieties in the Orhaneli Pluton reveal an adakitic nature (Altunkaynak et al., 2012) (Figure 10), whereas the northern belt generally represents calc-alkaline to high-K calc-alkaline rocks, except the Fıstıklı pluton, which shows tholeiitic affinity (Altunkaynak et al., 2012). In terms of geochemical features, plutons in the southern belt are very complex. In general, considering the plutonic rocks emplaced in the whole range of the Pontides, through time, starting from the Early Eocene to the Late Eocene, the nature of the magmatism changes from adakitic to nonadakitic magmatism (Topuz et al., 2005, 2011; Karlı et al., 2011; Eyüboğlu et al., 2011), except for some of the plutons intruded into the southern belt of NW Anatolia (Figure 10) (see Altunkaynak et al., 2012). When we compare Late Eocene Uludağ granite (Topuz and Okay, 2017) with the others, it is completely different in terms of normalized trace element and REE distributions (Figure 8), revealing an adakitic nature unlike most of the Late Eocene granitoids discussed above.

The volcanic equivalents of these Eocene plutons are generally distributed along the northern parts of the suture zone (Keskin et al., 2008; Kürkçüoğlu et al., 2008; Altunkaynak and Dilek, 2013; Ersoy and Palmer, 2013; Gülmez et al., 2013; Elmas et al., 2016; Kasapoğlu et al., 2016; Ersoy et al., 2017a, 2017b). Primitive mantle-normalized trace element distributions from the Ekmekçi granodiorite porphyry are similar to the volcanic rocks in general and deviate from the plutonic rocks in some trace elements such as Cs, Yb, and Lu (Figure 8). The chondrite-normalized REE element pattern of the Ekmekçi granodiorite porphyry is similar to some of the granitoids from both southern and northern plutons (see Figure 8). Furthermore, the REE pattern (Figure 8) almost perfectly matches the REE distribution field of the Nallıhan intermediate volcanics (Kasapoğlu et al., 2016). Early Eocene magmatism in the Eastern Pontides is adakitic in nature (Topuz et al., 2005, 2011; Karlı et al., 2010; Dokuz et al., 2013), whereas Early-Late Eocene volcanism in NW Anatolia reveals a nonadakitic signature

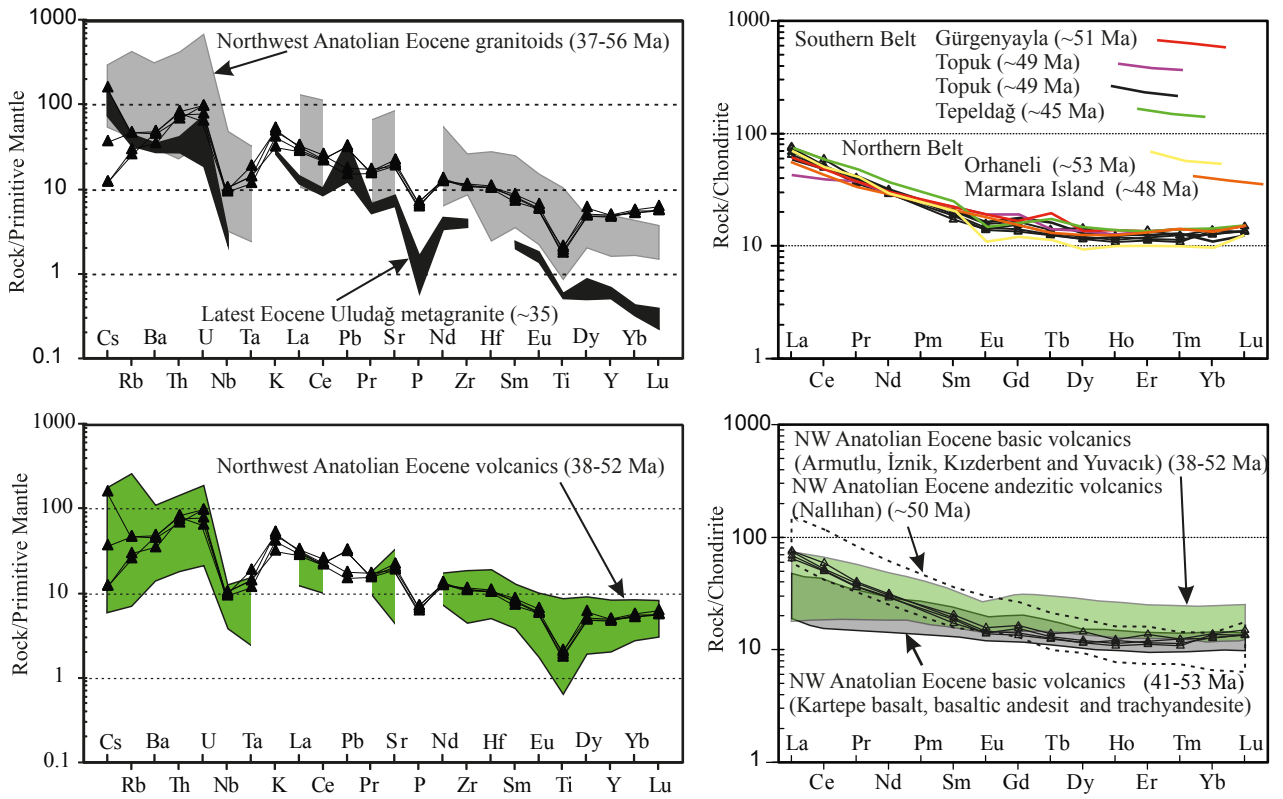


Figure 8. Multi-element spider and REE distribution of the samples from the Ekmekçi granodiorite porphyry. Normalization values are primitive mantle from Sun and McDonough (1989) and chondrite from Nakamura (1974). Note that there is no significant negative Eu anomaly. Source data presented as shaded area and individual element patterns are from Kürkçüoğlu et al. (2008), Altunkaynak et al. (2012), Altunkaynak and Dilek (2013), Gülmez et al. (2013), and Kasapoğlu et al. (2016).

Table 3. Sr-Nd isotopic data of the Ekmekçi granodiorite porphyry samples.

Sample	⁸⁷ Rb/ ⁸⁶ Sr	⁸⁷ Sr/ ⁸⁶ Sr	⁸⁷ / ⁸⁶ Sr (i)	¹⁴⁷ Sm/ ¹⁴⁴ Nd	¹⁴³ Nd/ ¹⁴⁴ Nd	¹⁴³ / ¹⁴⁴ Nd (i)	εNd (i)	TDM (Ga)
KG29	0.1269	0.705054(13)	0.70496	0.131654	0.512645(05)	0.512601	0.6	0.88
KG30	0.1239	0.704549(13)	0.70446	0.129480	0.512619(10)	0.512575	0.1	0.91
KG34	0.2091	0.704750(12)	0.70460	0.131759	0.512629(10)	0.512584	0.2	0.91
KG40	0.2321	0.704591(09)	0.70442	0.127670	0.512600(10)	0.512557	-0.3	0.92

Uncertainties for the ⁸⁷Sr/⁸⁶Sr and ¹⁴³Nd/¹⁴⁴Nd ratios are 2σ errors in the last two digits (in parentheses). Initial values are calculated for an assumed age of 51 Ma. εNd (i) values are calculated relative to CHUR with present day values of ¹⁴³Nd/¹⁴⁴Nd = 0.512638 and ¹⁴⁷Sm/¹⁴⁴Nd = 0.1967 (Jacobsen and Wasserburg, 1980). Nd model ages (TDM) are calculated with a depleted-mantle reservoir and present-day values of ¹⁴³Nd/¹⁴⁴Nd = 0.513151 and ¹⁴⁷Sm/¹⁴⁴Nd = 0.219 (e.g., Liew and Hofmann, 1988).

(Kürkçüoğlu et al., 2008; Gülmez et al., 2013; Elmas et al., 2016; Kasapoğlu et al., 2016; Ersoy et al., 2017a, 2017b), which is also similar to the central Pontides (Keskin et al., 2008; Göçmengil et al., 2018).

When we compare Nd and Sr isotope ratios of the Ekmekçi granodiorite porphyry with plutonic and volcanic rocks of NW Anatolia (Figure 9), all of the isotope ratios obtained from the Ekmekçi granodiorite porphyry are

similar to those of the mafic-intermediate volcanic rocks of NW Anatolia but are different than those from Eocene plutonic rocks (Figure 9).

The primitive mantle-normalized trace element patterns of the samples show enrichments in LILEs (Rb, Ba, Th, U, and K) relative to the high-field-strength elements (Ti, Hf, Zr, Nb, and Ta; Figure 8). The negative anomalies in Nb and Ta are characteristic of subduction-

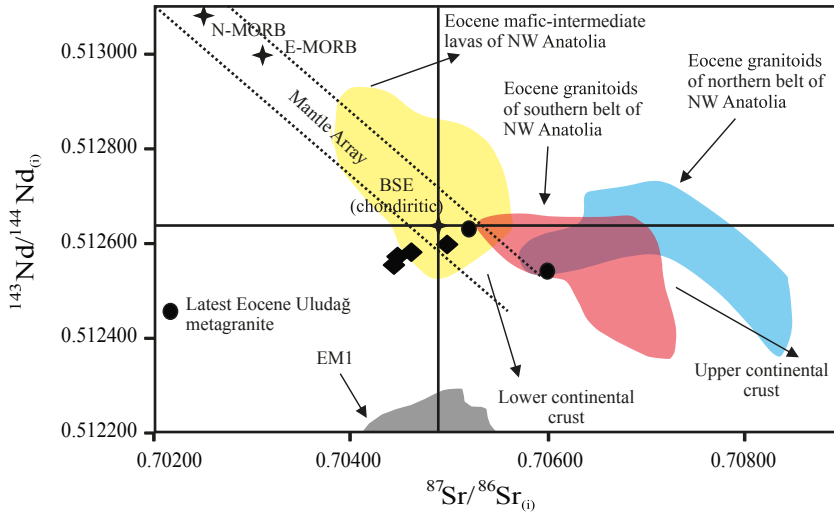


Figure 9. $^{143}\text{Nd}/^{144}\text{Nd}$ ($\epsilon_{\text{Nd}}(t)$) vs. $^{87}\text{Sr}/^{86}\text{Sr}$ ($\epsilon_{\text{Sr}}(t)$) diagram of the analyzed granodiorites (black diamonds). MORB and EM1 compositions are from Zindler and Hart (1986) and BSE (Bulk Silicate Earth) composition is from Hart et al. (1992). Sources: Kürkçüoğlu et al. (2008). Altunkaynak et al. (2012) and the references therein, Altunkaynak and Dilek (2013), Gülmez et al. (2013), Kasapoğlu et al. (2016), Topuz and Okay (2017).

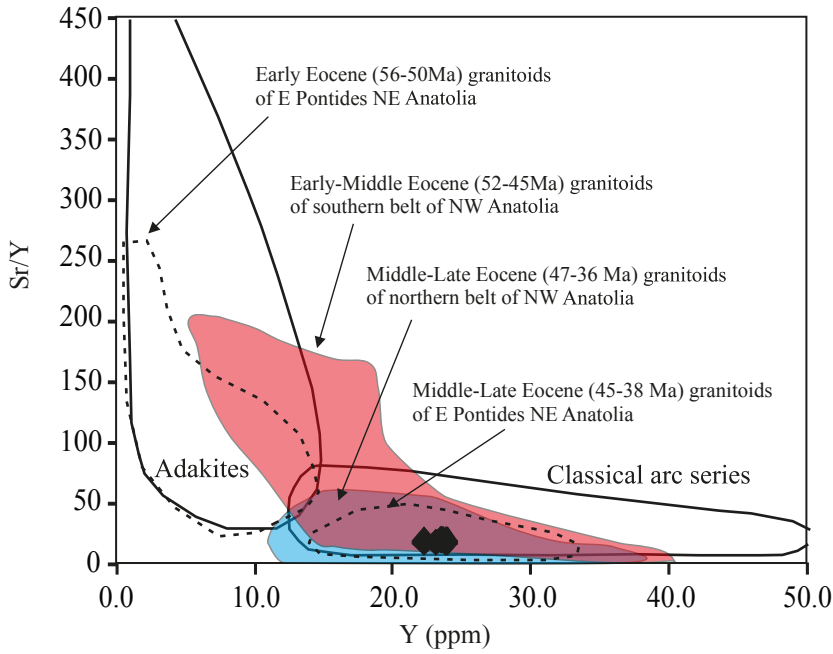


Figure 10. Sr/Y against Y plots indicating the classical arc nature of granodiorite porphyry samples from the Ekmekçi granodiorite (black diamonds). Fields for adakite and classical arc are taken from Martin et al. (2005). Sources: Topuz et al. (2005), Topuz et al. (2011), Karlı et al. (2011), Eyüboğlu et al. (2011), Altunkaynak et al. (2012) and the references therein.

related magmas, generally regarded as the influx of LILEs through slab dehydration (e.g., McCulloch and Gamble, 1991). The chondrite-normalized REE pattern of the samples has fractionated LREEs compared to

MREEs and HREEs. Furthermore, there is no significant fractionation between MREE and HREE profiles. The Eu anomaly in the REE pattern is generally a consequence of the fractionation of feldspar (Taylor and McLennan,

1985). The Ekmekçi granodiorite has a weak negative Eu anomaly (Eu/Eu^* is ~ 0.86 ; Table 2; Figure 8), which indicates minor plagioclase fractionation. Sr isotopes reveal depleted values with respect to the bulk Earth value, whereas Nd isotopes are enriched (Figure 9). This situation cannot be explained by only fractional crystallization and/or crustal contamination. The low ratio of Sr isotopes is not compatible with crustal contamination. Furthermore, $\epsilon\text{Nd}(i)$ values of the Ekmekçi granodiorite are between -0.3 and 0.6 , which are not compatible with other granitoids of ~ 52 Ma in NW Anatolia (Orhaneli and Gürgenyayla granitoids; Altunkaynak et al., 2012). Besides, the Nd-depleted mantle model (T_{DM}) values of the Ekmekçi granodiorite (0.88–0.92 Ga) are lower than those of the ~ 52 Ma granitoids (Orhaneli and Gürgenyayla; Altunkaynak et al., 2012). In particular, $^{87/86}\text{Sr}(i)$ values overlap with EM1 (enriched mantle) values (Figure 9). Taking all these features into account, it can be concluded that partial melting of subduction-modified lithospheric mantle through the upwelling of asthenosphere in a slab window (tear) contributed to the formation of the Ekmekçi granodiorite.

6. Conclusions

The Ekmekçi stock is a granodioritic intrusion in the northern belt of the postcollisional magmatic belt of NW

Anatolia. It displays a middle-Kcalc-alkaline metaluminous I-type signature and a narrow compositional variation. The Ekmekçi granodiorite porphyry has compositional features similar to those formed in subduction-related magmatic rocks at the active continental margins and postcollisional settings.

The Ekmekçi granodiorite porphyry is located in the northern belt of the NW Anatolian Eocene plutons, but in terms of the age span of the rocks, it is similar to the southern belt. When the geochemical characteristics and the ages of the Eocene magmatic rocks are considered, the Ekmekçi granodiorite porphyry is closely related to the NW Anatolian Eocene volcanic rocks rather than the plutonic rocks. Nd and Sr isotope ratios also reveal that it is similar to Eocene volcanic rocks in NW Anatolia and different from the Eocene plutonic rocks.

Acknowledgments

This study was supported by the Scientific and Technological Research Council of Turkey (TÜBİTAK, Project No: CAYDAG 111Y314). We thank W Siebel and E Reitter for their help with isotopic measurements. E Aydar and E Çubukçu are thanked for helping with CL imaging at Hacettepe University. We would like to thank M Kohut, I Peytcheva, and an anonymous reviewer for very careful and constructive reviews.

References

- Akdoğan R, Okay AI, Dunkl I (2018). Triassic-Jurassic arc magmatism in the Pontides as revealed by the U-Pb detrital zircon ages in the Jurassic sandstones of northeastern Turkey. *Turkish J Earth Sci* 27: 89-109.
- Altner D (1991). Microfossil biostratigraphy (mainly foraminifers) of the Jurassic-Cretaceous carbonate successions in northwestern Anatolia (Turkey). *Geol Romana* 27: 167-213.
- Altunkaynak Ş, Dilek Y (2013). Eocene mafic volcanism in northern Anatolia: its causes and mantle sources in the absence of active subduction. *Int Geol Rev* 55: 1641-1659.
- Altunkaynak Ş, Sunal G, Aldanmaz E, Genç CŞ, Dilek Y, Furnes H, Foland KA, Yang J, Yıldız M (2012). Eocene granitic magmatism in NW Anatolia (Turkey) revisited: new implications from comparative zircon SHRIMP U-Pb and $^{40}\text{Ar} - ^{39}\text{Ar}$ geochronology and isotope geochemistry on magma genesis and emplacement. *Lithos* 155: 289-309.
- Aysal N, Öngen AS, Peytcheva I, Keskin M (2012a). Origin and evolution of the Havran Unit, eastern Sakarya Basement (NW Turkey): new LA-ICP-MS U-Pb dating of the metasedimentary-metagranitic rocks and possible affiliation to Avalonian microcontinent. *Geodin Acta* 26: 1-25.
- Aysal N, Ustaömer T, Öngen S, Keskin M, Köksal S, Peytcheva I, Fanning M (2012b). Origin of the Early-Middle Devonian magmatism in the Sakarya Zone, NW Turkey: geochronology, geochemistry, and isotope systematics. *J Asian Earth Sci* 45: 201-222.
- Cavazza C, Federici I, Okay AI, Zattin M (2012). Apatite fission - track thermochronology of the Western Pontides (NW Turkey). *Geol Mag* 149: 133-140.
- Cavazza W, Okay AI, Zattin M (2009). Rapid early-middle Miocene exhumation of the Kazdağ Massif. *Int J Earth Sci* 98: 1935-1947.
- Çelebi D, Köprübaşı N (2014). The geochemical and Sr-Nd isotopic characteristics of Eocene to Miocene NW Anatolian granitoids: implications for magma evolution in a post-collisional setting. *J Asian Earth Sci* 93: 275-287.
- Dokuz A (2011). A slab detachment and delamination model for the generation of Carboniferous high potassium I-type magmatism in the Eastern Pontides, NE Turkey: Köse composite pluton. *Gondwana Res* 19: 926-944.
- Dokuz A, Uysal I, Siebel W, Turan M, Duncan R, Akçay M (2013). Post-collisional adakitic volcanism in the eastern part of the Sakarya Zone, Turkey: evidence for slab and crustal melting. *Contrib Mineral Petr* 166: 1443-1468.
- Duru M, Pehlivan S, Sentürk Y, Yavaş F, Kar H (2004). New results on the lithostratigraphy of the Kazdağ Massif in northwest Turkey. *Turkish J Earth Sci* 13: 177-186.
- Elmas A, Koralay E, Duru O, Schmidt A (2016). Geochronology, geochemistry, and tectonic setting of the Oligocene magmatic rocks (Marmaros magmatic assemblage) in Gökçeada Island, northwest Turkey. *Int Geol Rev* 59: 420-447.

- Ergül E, Gözler MZ, Akçaören F, Bilgi C, Dayıoğlu Ü, Öztürk Z, Tüzün RD, Yalçınkaya S (1986). *Bandırma - E6 paftası Jeoloji Haritası*. Ankara, Turkey: MTA Publications (in Turkish).
- Ersoy EY, Cüneyt A, Genç ŞC, Candan C, Palmer MR, Prelević D, Uysal İ, Regina MK (2017a). U-Pb zircon geochronology of the Paleogene-Neogene volcanism in the NW Anatolia: its implications for the Late Mesozoic-Cenozoic geodynamic evolution of the Aegean. *Tectonophysics* 717: 284-301.
- Ersoy EY, Palmer MR (2013). Eocene-Quaternary magmatic activity in the Aegean: implications for mantle metasomatism and magma genesis in an evolving orogeny. *Lithos* 180-181: 5-24.
- Ersoy EY, Palmer MR, Genç ŞC, Prelević D, Akal C, Uysal İ (2017b). Chemo-probe into the mantle origin of the NW Anatolia Eocene to Miocene volcanic rocks: implications for the role of subduction, slab roll-back and slab break-off processes in genesis of post - collisional magmatism. *Lithos* 288-289: 55-71.
- Eyüboğlu Y, Santosh M, Chung SL (2011). Crystal fractionation of adakitic magmas in the crust-mantle transition zone: petrology, geochemistry and U-Pb zircon chronology of the Seme Adakites, Eastern Pontides, NE Turkey. *Lithos* 121: 151-166.
- Göçmengil G, Karacık Z, Genç ŞC, Billor Z (2018). ^{40}Ar - ^{39}Ar geochronology and petrogenesis of postcollisional trachytic volcanism along the İzmir-Ankara-Erzincan Suture Zone (NE, Turkey). *Turkish J Earth Sci* 27: 1-31.
- Gülmez F, Genç SC, Keskin M, Tüysüz O (2013). A post-collision slab-breakoff model for the origin of the Middle Eocene magmatic rocks of the Armutlu-Almacık belt, NW Turkey and its regional implications. *Geol Soc Spec Publ* 372: 107-139.
- Harris NB, Kelley S, Okay AI (1994). Post-collision magmatism and tectonics in northwest Anatolia. *Contrib Mineral Petr* 117: 241-252.
- Hart SR, Hauri EH, Oschmann LA, Whitehead JA (1992). Mantle plumes and entrainment: isotopic evidence. *Science* 256: 517-520.
- Hejl E, Bernroider M, Parlak O, Weingartner H (2010). Fission-track thermochronology, vertical kinematics, and tectonic development along the western extension of the North Anatolian Fault zone. *J Geophys Res* 115: B10407.
- Irvine TM, Baragar WR (1971). A guide to the chemical classification of common volcanic rocks. *Canadian J Earth Sci* 8: 523-548.
- Jacobsen SB, Wasserburg GJ (1980). Sm-Nd isotopic evolution of chondrites. *Earth Planet Sci Lett* 50: 139-155.
- Karacık Z, Yılmaz Y, Pearce JA, Ece Öİ (2008). Petrochemistry of the south Marmara granitoids, northwest Anatolia, Turkey. *Int J Earth Sci* 97: 1181-1200.
- Karshi O, Dokuz A, Uysal İ, Aydın F, Kandemir R, Wijbrans J (2010). Generation of the Early Cenozoic adakitic volcanism by partial melting of mafic lower crust, Eastern Turkey: Implications for crustal thickening to delamination. *Lithos* 114: 109-120.
- Karshi O, Ketenci M, Uysal I, Dokuz A, Aydın F, Chen B, Kandemir R, Wijbrans J (2011). Adakite-like granitoid porphyries in the Eastern Pontides, NE Turkey: potential parental melts and geodynamic implications. *Lithos* 127: 354-372.
- Kasapoğlu B, Ersoy YE, Uysal İ, Palmer MR, Zack T, Koralay EO, Karlsson A (2016). The petrology of Paleogene volcanism in the Central Sakarya, Nallıhan Region: implications for the initiation and evolution of post-collisional, slab break-off related magmatic activity. *Lithos* 246: 81-98.
- Kaygusuz A, Arslan M, Siebel W, Sipahi F, İlbelly N (2012). Geochronological evidence and tectonic significance of Carboniferous magmatism in the southwest Trabzon area, eastern Pontides, Turkey. *Int Geol Rev* 54: 1776-1800.
- Keskin M, Genç ŞC, Tüysüz O (2008). Petrology and geochemistry of post-collisional Middle Eocene volcanic units in North-Central Turkey: evidence for magma generation by slab breakoff following the closure of the Northern Neotethys Ocean. *Lithos* 104: 267-305.
- Köprübaşı N, Aldanmaz E (2004). Geochemical constraints on the petrogenesis of Cenozoic I-type granitoids in Northwest Anatolia, Turkey: evidence for magma generation by lithospheric delamination in a post-collisional setting. *Int Geol Rev* 46: 705-729.
- Kürkçüoğlu B, Furman T, Hanan B (2008). Geochemistry of postcollisional mafic lavas from the North Anatolian Fault zone, Northwestern Turkey. *Lithos* 101: 416-434.
- Less GY, Özcan E, Okay AI (2011). Stratigraphy and larger foraminifera of the Middle Eocene to Lower Oligocene shallow-marine units in the northern and eastern parts of the Thrace Basin, NW Turkey. *Turkish J Earth Sci* 20: 793-845.
- Liew TC, Hofmann AW (1988). Precambrian crustal components, plutonic associations, plate environment of the Hercynian Fold Belt of Central Europe: Indications from a Nd and Sr isotopic study. *Contrib to Mineral Petr* 98: 129-138.
- Ludwig KR (2003). *User's Manual for Isoplot/Ex, Version 3.0. A Geochronological Toolkit for Microsoft Excel*. Berkeley Geochronology Center Special Publication No. 4. Berkeley, CA, USA: Berkeley Geochronology Center.
- Martin H, Smithies RH, Rapp R, Moyen JF, Champion D (2005). An overview of adakite, tonalite-trondhjemite-granodiorite (TTG), and sanukitoid: relationships and some implications for crustal evolution. *Lithos* 79: 1-24.
- McCulloch M, Gamble JA (1991). Geochemical and geodynamical constraints on subduction zone magmatism. *Earth Planet Sci Lett* 102: 358-374.
- Middlemost EAK (1985). *Magma and Magmatic Rocks: An Introduction to Igneous Petrology*. London, UK: Longman.
- Nakamura N (1974). Determination of REE, Ba, Fe, Mg, Na and K in carbonaceous and ordinary chondrites. *Geochim Cos Acta* 38: 757-775.
- Okay AI, Göncüoğlu CM (2004). The Karakaya Complex; a review of data and concepts. *Turkish J Earth Sci* 13: 77-95.
- Okay AI, Monié P (1997). Early Mesozoic subduction in the Eastern Mediterranean: Evidence from Triassic eclogite in northwest Turkey. *Geology* 25: 595-598.
- Okay AI, Özcan E, Hakyemez A, Siyako M, Sunal G, Kylander-Clark ARC (2019). The Thrace Basin and the Black Sea: the Eocene Oligocene marine connection. *Geol Mag* 156: 39-61.

- Okay AI, Satır M (2006). Geochronology of Eocene plutonism and metamorphism in northwest Turkey: evidence for a possible magmatic arc. *Geodin Acta* 19: 251-266.
- Okay AI, Satır M, Maluski H, Siyako M, Monie P, Metzger R, Akyüz S (1996). Paleo- and Neo-Tethyan events in northwest Turkey: geological and geochronological constraints. In: Yin A, Harrison M, editors. *Tectonics of Asia*. Cambridge, UK: Cambridge University Press, pp. 420-441.
- Okay AI, Satır M, Siebel S (2006). Pre-Alpide Palaeozoic and Mesozoic orogenic events in the Eastern Mediterranean region. *Geol Soc London Mem* 32: 389-405.
- Okay AI, Şengör AMC, Görür N (1994). Kinematic history of the opening of the Black Sea and its effect on the surrounding regions. *Geology* 22: 267-270.
- Okay AI, Tüysüz O (1999). Tethyan sutures of northern Turkey. *Geol Soc Spec Publ* 156: 475-515. Peccerillo A, Taylor SR (1976). Geochemistry of Eocene calc-alkaline volcanic rocks from the Kastamonu area, Northern Turkey. *Contrib Mineral Petr* 58: 63-81.
- Özdamar Ş, Sunal G, Demiroğlu M, Yaltrak C, Billor MZ, Georgiev S, Hames W, Dunkl I, Aydın HC (2018). Metamorphism, magmatism, and exhumation history of the Tavşanlı Zone, NW Turkey: new petrological constraints. *Turkish J Earth Sci* 27: 269-293.
- Peccerillo A, Taylor SR (1976). Geochemistry of Eocene Calc Alkaline Volcanic Rocks from Kastamonu Area, Northern Turkey. *Contrib Mineral Petr* 58: 63-81.
- Şengör AMC, Yılmaz Y (1981). Tethyan evolution of Turkey: a plate tectonic approach. *Tectonophysics* 75: 181-241.
- Şengün F, Koralay OE (2019). Petrography, geochemistry and provenance of Jurassic sandstones from the Sakarya Zone, NW Turkey. *Turkish J Earth Sci* 28: 603-622.
- Shand SJ (1943). *Eruptive Rocks, their Genesis, Composition, Classification, and their Relation to Ore-deposits, with a Chapter on Meteorites (Revised Second Edition)*. New York, NY, USA: John Wiley and Sons.
- Sun SS, McDonough WF (1989). Chemical and isotopic systematics of oceanic basalts: implications for mantle composition and processes. *Geol Soc Spec Publ* 42: 313-345.
- Sunal G (2012). Devonian magmatism in the western Sakarya Zone, Karacabey region, NW Turkey. *Geodin Acta* 25: 183-201.
- Sunal G, Erturaç, MK (2012). Estimation of the pre-North Anatolian Fault Zone pseudo-paleo-topography: a key to determining the cumulative offset of major post-collisional strike-slip faults. *Geomorphology* 159-160: 125-141.
- Taylor SR, McLennan SM (1985) *The Continental Crust: Its Composition and Evolution*. Oxford, UK: Blackwell.
- Topuz G, Altherr R (2004). Pervasive rehydration of granulites during exhumation - an example from the Pular complex, Eastern Pontides, Turkey. *Mineralogy and Petrology* 81: 165-185.
- Topuz G, Altherr R, Kalt A, Satır M, Werner O, Schwarz WH (2004). Aluminous granulites from the Pular complex, NE Turkey: a case of partial melting, efficient melt extraction and crystallization. *Lithos* 72: 183-207.
- Topuz G, Altherr R, Schwarz WH, Dokuz A, Meyer HP (2007). Variscan amphibolite-facies metamorphic rocks from the Kurtoğlu metamorphic complex (Gümüşhane area, Eastern Pontides, Turkey). *Int J Earth Sci* 96: 861-873.
- Topuz G, Altherr R, Schwarz WH, Siebel W, Satır M, Dokuz A (2005). Post-collisional plutonism with adakite-like signatures: the Eocene Saraycık granodiorite (Eastern Pontides, Turkey). *Contrib Mineral Petr* 150: 441-455.
- Topuz G, Altherr R, Siebel W, Schwarz WH, Zack T, Hasözbeğ A, Barth M, Satır M, Şen C (2010). Carboniferous high potassium I-type granitoid magmatism in the Eastern Pontides: the Gümüşhane pluton (NE Turkey). *Lithos* 116: 92-110.
- Topuz G, Okay AI (2017). Late Eocene-Early Oligocene two-mica granites in NW Turkey (the Uludağ Massif): water-fluxed melting products of a mafic metagraywacke. *Lithos* 268-271: 334-350.
- Topuz G, Okay AI, Altherr R, Schwarz WH, Siebel W, Zack T, Satır M, Şen C (2011). Post-collisional adakite-like magmatism in the Ağvanis Massif and implications for the evolution of the Eocene magmatism in the Eastern Pontides (NE Turkey). *Lithos* 125: 131-150.
- Topuz G, Okay AI, Schwarz WH, Sunal G, Altherr A, Kylander-Clark ARC (2018). A middle Permian ophiolite fragment in Late Triassic greenschist- to blueschist-facies rocks in NW Turkey: an additional pulse of suprasubduction-zone ophiolite formation in the Tethyan belt? *Lithos* 300-301: 121-135.
- Tüysüz O, Dellaloğlu AA (1992). Geologic evolution of Cankiri and its tectonic units. In: *Türkiye 9. Petrol Kongresi Bildiriler*, pp. 333-349 (in Turkish with English abstract).
- Tüysüz O, Dellaloğlu AA, Terzioğlu N (1995). A magmatic belt within the Neo-Tethyan suture zone and its role in the tectonic evolution of northern Turkey. *Tectonophysics* 243: 173-191.
- Ustaömer PA, Ustaömer T, Collins AS, Reischpeitsch J (2009). Lutetian arc-type magmatism along the southern Eurasian margin: new U-Pb LA-ICPMS and whole-rock geochemical data from Marmara Island, NW Turkey. *Miner Petrol* 96: 177-196.
- Ustaömer PA, Ustaömer T, Robertson AHF (2012). Ion Probe U-Pb dating of the Central Sakarya basement: a peri-Gondwana terrane intruded by late Lower Carboniferous subduction/collision-related granitic rocks. *Turkish J Earth Sci* 21: 905-932.
- Zindler A, Hart S (1986). Chemical geodynamics. *Annual Rev Earth Planet Sci Lett* 14: 493-571.